

FORMATION OF THREE-DIMENSIONAL STRUCTURES OF METAL NANOPARTICLES IN ALKALI-HALIDE CRYSTALS USING INTERFERENCE LIGHT FIELD

A. V. TYURIN, S. A. ZHUKOV*, AND A. Y. BEKSHAEV

Physics Research Institute, Odesa I.I. Mechnikov National University, V. Zmianka 2, 65082, Odesa, Ukraine

*Corresponding author: zhukov@onu.edu.ua

Received: 28.06.2025

Abstract. Rapid progress in high technologies requires the implementation of new methods for recording, reproducing, and converting electromagnetic radiation in the visible and near-infrared ranges. Among those, of particular relevance is the problem of creating regular 3D arrays of nanoscale objects in condensed media and controlling their properties, structure, and topology. Such nanoobjects and their arrays offer efficient means for controllable data encoding and information recording. In particular, these can be created in materials based on additively colored alkali halide crystals (ACAHCs) containing *F*-centers. The advantages of these media are as follows: (i) nano-objects of very diverse structures and properties can be formed; (ii) the spatial distribution of quasi-metallic *X*-centers created in the ACAHC volume due to the *F*-*X* transformation of color centers under the action of the spatially inhomogeneous interference light field (ILF) completely reproduces its spatial structure. As a result, changing the ILF configuration in the ACAHC volume enables control of the spatial structure formed by the *X*-centers. The methods for controlling the spatial distribution of *X*-centers have been tested in holographic practice and confirmed by modeling results. They can serve as a prototype for a wide range of procedures for the purposeful generation of structures from nanoparticles emerging as products of photolysis in the crystal volume.

Keywords: alkali halide crystals; *F*-centers; *X*-centers; interference light field; Demer effect; quasi-metallic nanoparticles; 3D arrays

UDC: 535.37

DOI: 10.3116/16091833/Ukr.J.Phys.Opt.2025.03043

This work is licensed under the Creative Commons Attribution International License (CC BY 4.0).

1. Introduction

Nanoscale objects, particularly metallic nanoparticles, exhibit unique and still insufficiently studied features that are fundamentally different from the properties of both molecules and macroscopic bodies. These special features are most clearly manifested in the behavior of 1D, 2D, and 3D arrays (threads, surfaces, superlattices, etc.) of such particles formed in the bulk of dielectric or semiconductor materials [1]. Particular attention is attracted to their electronic and optical properties, which form the base for the future creation of new electronic and optoelectronic elements [2]. Therefore, the search for new and the improvement of existing methods for the purposeful formation of 3D arrays of metallic nanoparticles in the bulk of a condensed medium is an urgent technological problem. A special interest is associated with the optical approaches for creating such structures, whose potential abilities originate from the fact that many materials respond well to photo-exposure [1–4].

In this regard, materials used for the hologram recording are of special interest due to their exclusive response to highly structured optical fields. In the holographic practice, three types of photosensitive media are known that can be essential for the further development of

the described ideas. These are: (i) alkali-halide crystals containing colloid nano-scale centers of alkali metals, (ii) silver-containing glasses, and (iii) glass-like chalcogenide semiconductors. In this work, our consideration relates to materials of the 1st category, represented by additively colored alkali-halide crystals (ACAHCs) containing quasi-metallic color centers (F -centers) [3–5]. The physical characteristics of F -centers as well as their spatial distribution are highly sensitive to the electromagnetic radiation, and can be controlled and regulated by exposition to the properly formed structured light field with specially adjusted spatial, polarization, or dynamical characteristics [6,7]. Specifically, regular 3D structures can be formed with quasi-metallic nanocenters (NCs) of a special type (X -centers), originating from F -centers due to the light-induced F - X transformation [3,4]. In the presence of a spatially inhomogeneous light field, X -centers can be formed with a wide range of sizes, spanning from atomic to micrometer scales. Noticeably, the resulting spatial distribution of the X -centers is regulated by the spatial structure of the illuminating light field. Accordingly, one obtains a simple way to control the spatial distribution of X -centers in the ACAHC, which form the basis for the creation of optoelectronic devices of a fundamentally new class [5].

2. Problem description and experimental approach

To successfully realize the possibilities mentioned above, it is necessary to know the mechanism of the structured-light-stimulated photothermal F - X transformation in ACAHCs. The main difficulty of studying this mechanism is that, while in a uniform light field the coagulation of F -centers into X -centers occurs directly due to photodiffusion, in the presence of inhomogeneous illumination, local electric fields arise, which, additionally, induce the centers' drift [8].

Let us consider the simplest situation where the inhomogeneous illumination is supplied by the interference light field (ILF): a superposition of two plane waves of equal intensities propagating along the axes making a certain angle with each other (Fig. 1). The existence of local electric fields in the ILF-illuminated ACAHC is caused by the following reasons. During photoionization of F -centers in illuminated places (antinodes) of the ILF, free electrons and positively charged mobile anion vacancies (α -centers) arise, which diffuse into unlit places (nodes) of the ILF. In this process, since the diffusion coefficients of electrons

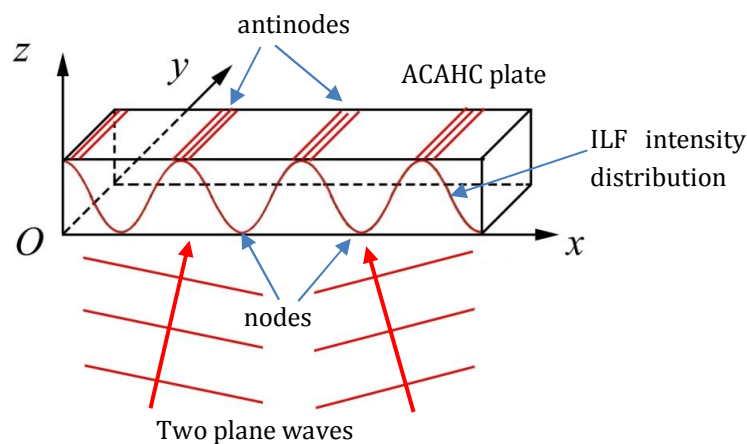


Fig. 1. Scheme of the ILF formation and the ACAHC plate location with respect to the coordinate frame.

and α -centers are different, local electric fields arise in the volume between the maxima and minima of the ILF intensity (this is analogous to the known Demer effect [9]). These local electric fields have a significant impact on the photothermal F - X transformation process. As shown in [10], this process comprises three stages.

At the first stage, the F -centers in the nodes of the ILF distribution remain unchanged, and in the antinodes, they coagulate into X -centers. The resulting spatial inhomogeneity in the distribution of F - and X -centers in the ACAHC volume leads to spatial modulation of the absorption and refraction coefficients, which reproduces the spatial structure of the ILF and can be considered as a diffraction grating. This diffraction grating in the entire visible range of the spectrum is predominantly of the amplitude character (since the absorption bands of the F - and X -centers (Fig. 2) are sufficiently close to each other and overlap). The diffraction efficiency (DE) of the obtained diffraction gratings across the entire visible spectrum is low, ranging from 1% to 3%.

At the second stage, the coagulation of F -centers into X -centers also occurs in the ILF nodes, and the difference in spatial distribution between F - and X -centers over the ACAHC volume disappears. Thermodynamic equilibrium is established between the F - and X -centers throughout the entire volume of the crystal, which is characterized by a significant predominance of the concentration of X -centers compared to F -centers. This occurs for the following reasons. First, since the ILF is obtained as a superposition of two plane light waves, the resulting light intensity is modulated sinusoidally in space; it vanishes only in the ILF nodes and only if the intensities of the superimposed beams are strictly equal, which is quite difficult to realize in practice. Additionally, light scattering is possible, which also results in non-zero illumination in the ILF nodes. Consequently, non-zero intensity exists even in the ILF nodes, which is naturally coupled with the formation of X -centers. In the regions of highest X -centers' concentration (X -lines), the light absorption reaches a maximum, and the DE falls to zero. The process of X -line formation is illustrated in Fig. 2, where the absorption spectrum of a crystal region, initially typical of F -centers (curves 1), changes with increasing illumination time to the form characteristic of X -centers (curves 3, 4) [10–12].

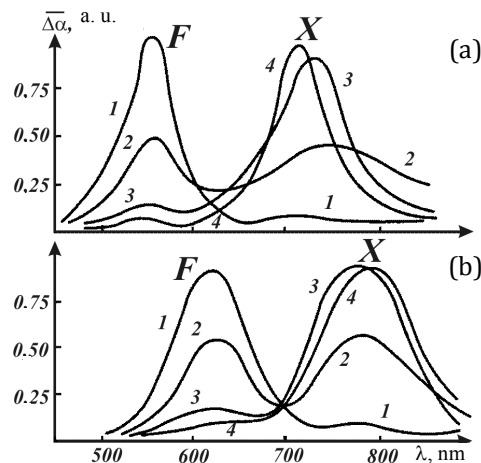


Fig. 2. Spectral dependencies of the mean absorption $\overline{\Delta\alpha}$ in the X -line of the grating registered (a) at the temperature ~ 200 °C in the additively colored crystals KBr, and (b) at ~ 280 °C in the additively colored KCl, for different registration moments after the start of illumination t (s): (1) 0; (2) 20; (3) 30; (4) 500.

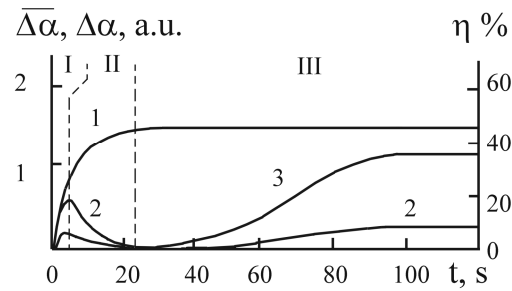


Fig. 3. Main processes associated with F - X transformation in an additively colored crystal KCl at the temperature 280 °C, illuminated by ILF with $\lambda = 632$ nm [12]: (1) evolution of the mean absorption $\overline{\Delta\alpha}$ in an X -line; (2) evolution of the absorption index $\Delta\alpha$ (determined according to the methods of measurement of the amplitude and phase grating components [4]) in the ILF nodes; (3) evolution of the DE η . Time intervals I, II, III, separated by vertical dashed lines, correspond to the 1st, 2nd, and 3rd stages of the photothermal F - X transformation.

At the third stage, the redistribution of the F - and X -centers between the nodes and antinodes of the ILF takes place, as a result of which almost all NCs, both of F - and X -types, are concentrated in the ILF nodes, while in the antinodes, NCs are absent, i.e., layers of discolored crystal are formed. Such a sort of diffraction grating in the wavelength range of 400-650 nm is predominantly of the phase nature, and its DE at the He-Ne laser wavelength reaches 40%. The dynamics of slowly increasing DE at this stage, which reflects the redistribution of NCs between ILF nodes and antinodes, have an S-shaped character (Fig. 3, curve 3), indicating a fundamentally new mechanism of the F - X transformation in ACAHC compared to previously studied ones.

Thus, the mechanism of photothermal F - X transformation under the action of structured light in ACAHC is indeed fundamentally different from the mechanism of F - X transformation under the action of uniform illumination. This is especially evident during the third stage, when the process of NCs' redistribution between the nodes and antinodes of the ILF occurs, leading to the complete bleaching of the crystal in the ILF antinodes. Until now, the mechanism of F - X transformation in ACAHC under the action of inhomogeneous illumination has not been studied. A detailed investigation of such a complex process requires not only experimental study but also theoretical justification, which, as will be shown below, is significantly hindered due to the complexity of the process. Therefore, in the present work, we employ the computer simulation of this process. Previously, the usefulness of numerical simulation in studying phenomena associated with transformations induced by structured light in ACAHC has been demonstrated [11]. In this work, we present the continuation and further development of this method.

3. Numerical model and computer simulation

3.1. General consideration

Computer modeling assumes the following model conditions. Let a plane-parallel plate of the ACAHC containing only F -centers be placed in the ILF, whose intensity I changes only along the x -coordinate according to the law (see Fig. 1)

$$I(x) = \frac{I_0}{2} \left(1 + \cos \frac{2\pi}{d} x \right), \quad (1)$$

where d is the period of the ILF spatial oscillations, and I_0 is the maximum ILF intensity. The ribs of the ACAHC plate are oriented along the coordinate axes (x, y, z) (Fig. 1). The plate thickness along the z -axis and its absorption coefficient are so small that the interfering waves practically do not weaken, and the formula (1) is valid throughout the whole plate. Under the influence of light, electrons are released from the F -centers into the conduction band of the ACAHC. The process of the F -centers photoexcitation evolves in two stages: after the absorption of a photon by the F -center, an excited F^* -center is first formed, for which the

electron energy is approximately 0.2 eV below the conduction band bottom, and afterwards, the electron is thermally excited to the conduction band. In turn, the release of electrons from the F -centers leads to the emergence of mobile positively charged α -centers whose concentration is equal to that of free electrons.

The described process of F -centers' photoexcitation can be modeled by the following differential equations [4,12]:

$$\frac{dn}{dt} = \beta^* N^* - \gamma_h n(n + n_i) - \frac{dn_i}{dt}, \quad (2)$$

$$\frac{dN^*}{dt} = \delta \frac{I}{\hbar\omega} (N - N^* - n_i - n) - N^* (\gamma_h^* + \beta^*), \quad (3)$$

$$\frac{dn_i}{dt} = \gamma_i n(N_i - n_i) - \beta_i n_i. \quad (4)$$

Here n , N , N^* , N_i , n_i are, respectively, the concentrations of free electrons, F -centers, F^* -centers, traps for free electrons and electrons captured by them; β^* , γ_h^* are the probabilities of thermal ionization and recombination of the F^* -center, γ_h is the probability of recombination of an electron with a free α -center, γ_i and β_i are the probabilities of capture of a free electron by a trap and its thermal excitation back into the conduction band, δ is the cross section of photon capture by the F -center, $I/\hbar\omega$ is the flow density of quanta of the exciting light (see Eq. (1)) with the frequency ω , \hbar denotes the Planck constant.

The electrons and α -centers released after photoexcitation of the F -centers diffuse from the highly illuminated regions of the plate to the less illuminated ones. Due to the difference in the diffusion coefficients of the electrons D_n and of the α -centers D_h , local electric Dember fields arise between the maximally and minimally illuminated regions of the ACAHC; the electric field strength E is determined by the expression [9]

$$E = -\frac{kT}{e} \frac{D_n - D_h}{n_0 D_n + p_0 D_h} \frac{dn}{dx}, \quad (5)$$

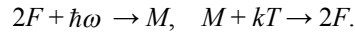
where k is the Boltzmann constant, T is the absolute temperature, e is the electron charge absolute value, n_0 and p_0 are the concentrations of electrons and α -centers in the absence of illumination.

Local electric fields slow down the diffusion of more mobile charge carriers (in our case, electrons) and, due to drift, accelerate less mobile charge carriers (α -centers). During diffusion, α -centers can localize near the F -center and, after capturing an electron, form a stable combination of two F -centers – the M -center [3]. In turn, the M -center, after several successive captures of electrons and α -centers, forms an aggregate center consisting of a large number of F -centers, i.e., the X -center [3].

We do not take into account the capture of electrons by the F -centers with the formation of the F' -centers [3], since their concentration is insignificant at room temperature. However, the role of electron traps must be considered, since in the presence of their sufficient number, both the dynamics and the stationary value of the free electrons' concentration vary significantly, due to the change in the nature of recombination from bimolecular to monomolecular.

It is also necessary to take into account the change in the concentration of F -centers: (a) its decrease due to aggregation and (b) an increase as a result of thermally- and charge-

stimulated dissociation of aggregate centers into the original F -centers. If aggregation stops at the M -center stage, these reactions proceed in accordance with the formulas



If the aggregate centers consist of a larger number of F -centers, the chain of formulas is correspondingly extended. If we additionally take into account the dynamic change in the light intensity due to its absorption in the crystal volume, this will further complicate the system of equations. It is very difficult to find an analytical solution to the system (2) – (4) in a non-uniform light field $I(x)$, where one should keep in mind the geometry of the light intensity distribution and the dynamically changing Dember field distribution, distributions of the initial F -centers ΔN and the aggregate X -centers ΔN_X . Under such conditions, the only way to solve the problem is through numerical simulation. Despite the conventionality of this approach, it enables the identification of the characteristic features of the photoinduced processes, the conditions for their implementation, and the comparison of the obtained results with the experimental data.

The simulation was performed in the DELPHY environment using the Monte-Carlo method. The objects of simulation were the Dember field and the concentrations of quasi-metallic NCs and intermediate products of their synthesis. The special attention was paid to variations of these quantities over the crystal volume and to the dynamics of their changes in time, as functions of the ILF spatial frequency, the crystal temperature, and other external parameters (Fig. 4).

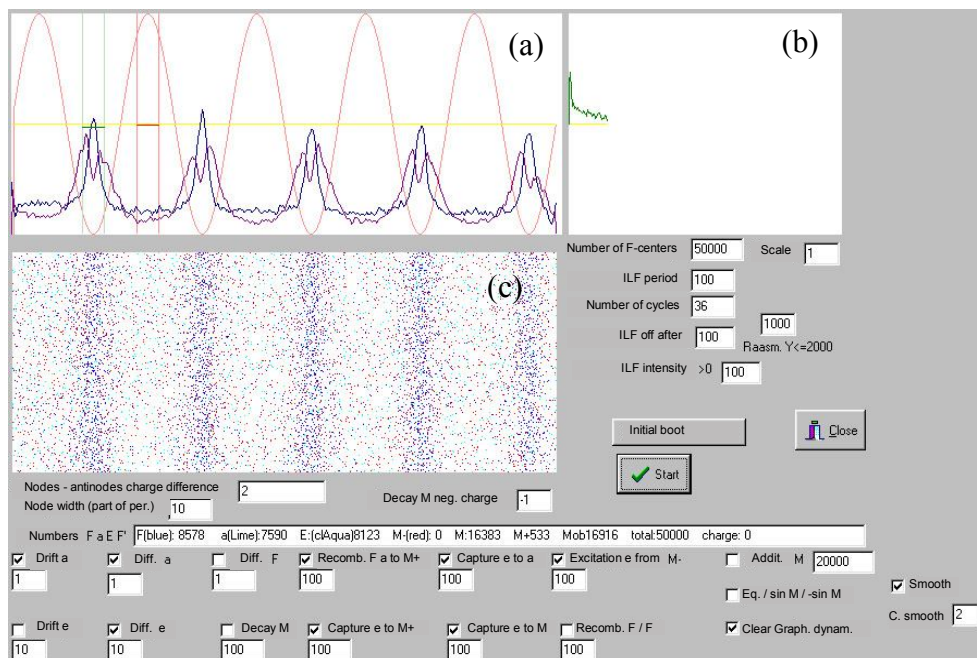


Fig. 4. General view of the program interface: (a) Spatial distribution of the ILF (red), concentration of F -centers N (blue) and of the aggregate X -centers N_X (magenta) along the x -coordinate in the crystal; horizontal yellow and green lines denote the mean value of the ILF intensity and the mean value of the grating absorption; (b) Kinetics of modulation of the mean value of the grating absorption (green) at the locations shown in (a) by vertical green lines; (c) 2D section of the distributions of F -centers (blue), aggregate centers (magenta), α -centers (cyan), electrons (red).

The following assumptions were made during the modeling:

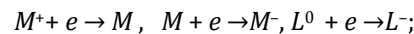
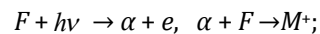
1. The ACAHC samples have an insignificant thickness, such that the change in light intensity across the sample thickness can be neglected.
2. *F*-centers and aggregate centers are localized, and only α -centers and free electrons possess mobility (both for the drift and diffusion).
3. Only *F*-centers are photoactive.
4. The aggregation process stops at the stage of *M*-centers (*2F*-centers), which imitaty *X*-centers in this model.
5. The role of electron traps can be played by both aggregate centers and additional centers uniformly distributed throughout the crystal, which do not participate in photochemical reactions.

All these approximations are quite close to the real conditions of our experiments. However, during the process of further development, the codes will be refined to make the numerical model more closely align with the actual physical conditions.

Therefore, the following objects participate in this model:

1. Photons.
2. Neutral *F*-centers and positively charged α -centers.
3. *M*-centers in three charge states: M^+ , M^0 , M^- .
4. Electrons.
5. Electron traps. These can be some additional (alien) *L* centers in the states L^0 and L^- , or the aggregate centers themselves, if the state M^- is allowed for them.

Each object was assigned a set of properties: diffusion and drift coefficients, the nature of their interaction with light, electric field and with each other (the possibility of fusion or decay, which causes the formation of new centers, or a change in the charge state with the release or capture of electrons). The following possible reactions were considered:



(the symbol kT means that the reaction requires a thermal excitation). The system parameters of Eqs. (2)–(5) may vary in a wide range; during the simulation, we accepted the values reported in the literature as characteristic for KCl crystals [3,4,12]. Additionally, whenever possible, the calculations were performed in relative units.

When constructing a model closer to reality, in which the aggregation products are not M^- , but *X*-centers, the coefficient 2 in the last row of the above reactions should be increased by at least an order of magnitude, and all intermediate aggregate centers should be taken into account: R_3 -centers (complex of three *F*-centers), R_4 -centers (complex of four *F*-centers), etc. In each calculation cycle, changes in the concentrations of NCs were first determined in accordance with the local Eqs. (2)–(4), after which the redistribution of NCs and free electrons over the sample due to diffusion and drift was evaluated in accordance with concentration gradients and the local electric fields, via using Eq. (5) and its analogs.

During the modeling, the main task was set to reproduce the experimentally observed phenomena [13] and to elucidate the conditions for their manifestation.

3.2. Modeled phenomenon: an S-shaped increase in the DE of a spatially periodic structure of NCs (SPSNC)

According to the proposed diffusion-drift mechanism, the production of electron traps during coagulation ensures an S-shaped increase of the SPSNC DE, and, consequently, of the concentration of NCs that form the SPSNC. We tried to achieve similar results using a numerical code. The models were built in 2 versions. In the first one, there were no electron traps, or these were some alien L -centers with a time-independent concentration N_L , uniformly distributed over the crystal volume; in the second, the traps are the final reaction products, M -centers. The corresponding modifications were introduced in the kinetic Eqs. (2)–(4). Note that under the conditions of spatially periodic ILF illumination, the main model parameters also show spatially periodic distributions; for simplicity, in the following illustrations, these are described by some characteristic values, e.g., the Dember field strength is characterized by its maximum absolute value E_m .

The calculation results confirm the correctness of the model concepts presented above. In the absence of electron capture by aggregate centers, diffusion-drift processes can quite well ensure the concentration of the aggregate centers in the ILF minima, but do not explain the S-shaped nature of the kinetics of the Dember field modulation and of the concentration of NCs that form the SPSNC (Fig. 5a).

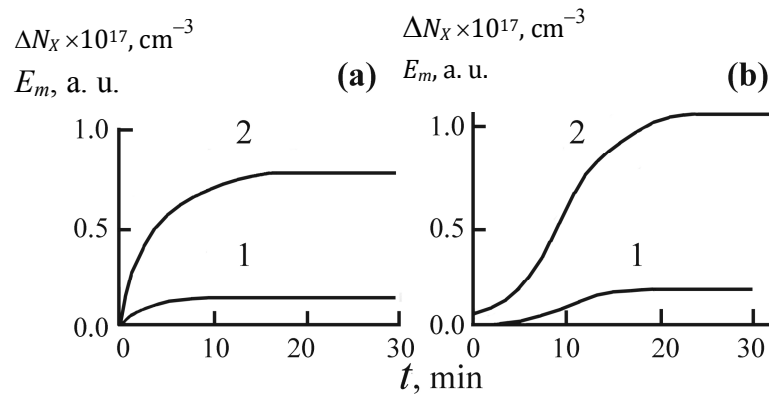


Fig. 5. Kinetics of change in (1) maximum Dember field absolute value E_m and (2) modulation of aggregate centers' concentrations ΔN_x calculated under suppositions: (a) electron traps are uniformly distributed over the crystal, (b) electron traps are the aggregate centers.

In contrast, allowance for the electrons' capture by aggregate centers directly leads to the S-shaped kinetics of the electric field and concentration of NCs that form the SPSNC. In this case, the charge concentrated on the traps is greater in places where the traps' density is higher, i.e., in the nodes. This increases the electric field strength between the minima and maxima of the ILF and accelerates the drift of α -centers to the minima, where they coagulate, forming new traps. Thus, a positive feedback mechanism is implemented, which stipulates the S-shaped growth of the difference in the concentrations of aggregate centers ΔN_x and the Dember field modulation E_m (Fig. 5b).

Consequently, it can be concluded that these results of computer modeling confirm the assumption that the traps are the X -centers themselves. Additional experimental confirmation of the correctness of this conclusion can be found in [14], where it is shown that fairly deep traps (~ 0.4 eV) can be present in the ACAHC, and their concentration increases during the crystal illumination, i.e., they are just the aggregate centers.

3.3. Modeled phenomenon: the almost complete displacement of X -centers from the areas of maximum illumination to the areas of minimum illumination

To obtain such a redistribution within our model framework, it is necessary to add the mechanism of the aggregate centers' destruction in the regions of illumination maxima to the mechanisms considered in the previous paragraph. As the results of modeling show, taking into account only their thermal instability is not sufficient. Therefore, we employed the assumption of charge instability of X -centers: a negative charge makes them stable, a positive charge – unstable. The kinetics of NCs redistribution obtained in this case are the closest to the experimental ones (Fig. 5b), and it is possible to obtain almost complete concentration of NCs in the minima of the ILF, while in the maxima, layers of the discolored crystal remain.

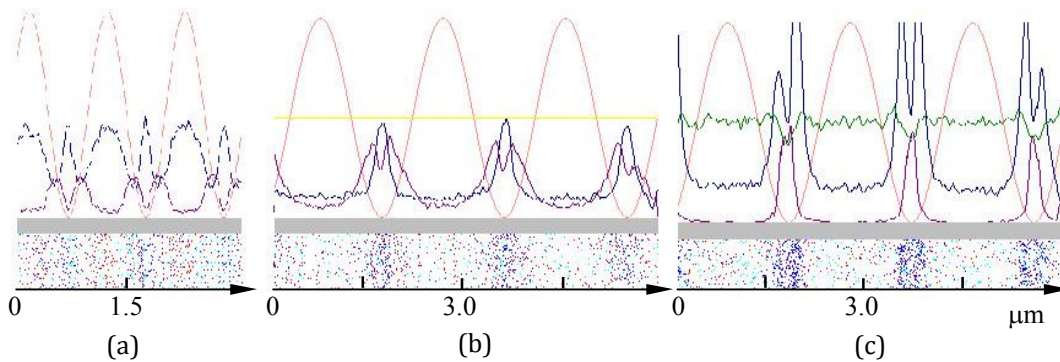


Fig. 6. Distributions of NCs on the background of the ILF intensity distribution under various conditions of the SPSNC formation. The meaning of colors is the same as in Fig. 4; further explanation see in the text.

Fig. 6 shows characteristic examples of the spatial distributions of the F -centers N (blue curves), X -centers N_x (magenta curves), and of the grating absorption $\Delta\alpha$ (green curve in Fig. 6c). In Fig. 6a, the situation is presented where only the 1st stage of the F - X transformation is realized (see Section 2), and the X -centers are not traps for electrons. In Fig. 6b, the almost optimal conditions are realized [15]: the considered mechanism of the SPSNC formation induces almost complete displacement of X -centers from the regions of illumination maxima to the ILF minima. In the situation of Fig. 6b, like in Fig. 6c, the 3rd stage of the F - X transformation is completed, the X -centers act as efficient electron traps. However, the specific sets of generation-recombination parameters in Eqs. (2) – (4) in cases (b) and (c) are different, which causes qualitatively different consequences: in case (b), additional maxima appear in the distribution of N_x (magenta) while in case (c), the distribution of N_x preserves the periodicity of the ILF but additional maxima of N emerge. In more detail, these features will be discussed in the special Section 3.5 below.

3.4. Modeled phenomenon: threshold nature of the SPSNC formation

Since X -centers are destroyed not only through thermal excitation, but also due to the induced Dember electric field (Eq. 5) (which causes the X -centers charging with an effective positive charge), it is natural to assume the presence of a threshold value of the electric field strength, above which the balance of diffusion and drift flows is disrupted, and the process of the NCs' redistribution between the ILF maxima and minima is sharply accelerated. The value of the Dember field can be controlled by adjusting the intensity of the light waves forming the periodic ILF pattern. The results of numerical calculations correlate with

experimental data and fully confirm the assumption of the existence of a critical value of the local Dember field strength, and, accordingly, of the existence of a critical (threshold) value of the ILF intensity, after which the SPSNC formation acquires a qualitatively different character, with complete redistribution of the X -centers to the ILF nodes (Fig. 6c).

3.5. Modeled phenomenon: the shape of the spatial distribution of the concentration of F - and X -centers (profile of the grating line)

As was noted in Section 3.3, by varying the model parameters, one may find the situations where the distribution of NCs with respect to the ILF grating shows special forms (Fig. 6). For example, Fig. 6a illustrates the case where the spatial distribution of F -centers (blue curves) and X -centers (magenta curves) have two maxima within a single ILF period, and the positions of maxima for F -centers differ from those for X -centers. In Fig. 6b, the curve corresponding to F -centers has one maximum, whereas the distribution of X -centers shows two maxima within a single period; Fig. 6c illustrates a similar, but directly opposite situation.

This can be interpreted as the emergence of additional periodic SPSNC distributions with spatial frequencies differing from the ILF spatial frequency by a factor of m . Depending on the model parameters, entering Eqs. (2)–(5), the number m may vary within rather wide limits and can even be fractional. The obtained result can be considered as evidence of the multifrequency character of the formed SPSNC, which has never been observed before. This result of modeling (obtained exclusively from numerical calculations) was confirmed experimentally.

It can be seen from the character of diffraction of an external plane wave, incident on the KCl plate with the light-induced SPSNC grating (Fig. 7). In the course of the light-induced F - X transformation, additional diffraction maxima appear, indicating the formation of numerous additional “multigratings” (Fig. 7, grey columns). The formation of “multigratings” is rather expressive at the intermediate stages of the photothermal F - X transformation. But with increasing exposure, the multifrequency effect smoothed out, m approached 1, which corresponds to the destruction of additional concentration maxima of the SPSNC and an increase of the main maximum, coinciding in spatial frequency with the spatial frequency of the ILF (Fig. 7, black columns; Fig. 8).

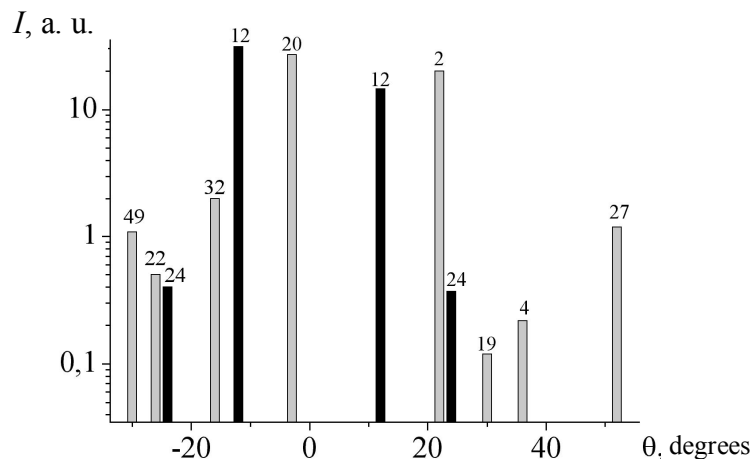


Fig. 7. Histogram of the diffraction maxima intensities depending on the angle θ of incidence of the external light beam (wavelength $\lambda = 632.8$ nm). Black columns characterize the maxima observed when the diffraction angle and the incidence angle coincide and are equal to the Bragg or double-Bragg values [4]. For grey columns, the angles of incidence and diffraction differ, which corresponds to the additional “multigrating” diffraction. The number above each column denotes the diffraction angle, and the column height is proportional to the intensity.

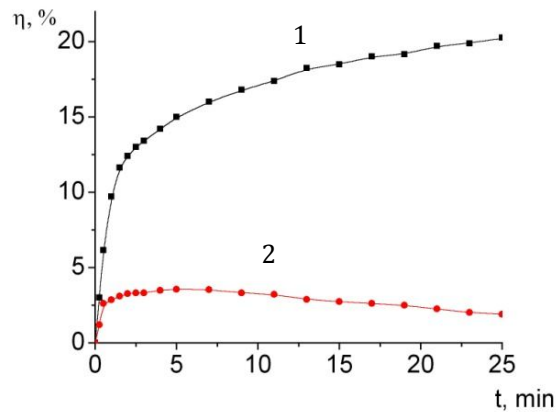


Fig. 8. Kinetics of changes of the DE η in the diffraction maxima: (1) main maximum (one of the black columns in Fig. 7), the angle of incidence is equal to the Bragg angle; (2) one of the side maxima (grey column of Fig. 7), the angle of incidence $\theta = 22^\circ$.

3.6. Modeled phenomenon: the use of time-dependent light structures for moving NCs across a crystal

The temporal evolution of the ILF in the ACAHC volume (at a speed not exceeding the characteristic speed of the NCs' redistribution) induces the associated waves of moving NCs in the crystal. In other words, the dynamic formation of SPSNC can be realized and controlled via the dynamic variations of the ILF configuration. For example, the following situation was analyzed within the frame of our model: The initial ILF of the spatial period $d = 1.8 \mu\text{m}$ was illuminating the ACAHC during 10 min, after which the interference pattern was set in the x -directed motion with the uniform velocity of 1.5 nm/s (thus performing approximately one-period shift during each 20 minutes). Such a controllable spatial motion of the ILF can be practically realized, e.g., via the regular change in the phase difference between the interfering plane waves in the scheme of Fig. 1.

Fig. 9 shows the distribution of NCs in the crystal volume near the right edge of the ACAHC plate (see Fig. 1) calculated for the time moment $t = 30$ min after the ILF motion started. It confirms that the movable ILF illumination leads to progressive displacement and specific relocation of the NCs, with essential modification of their spatial distribution. In particular,

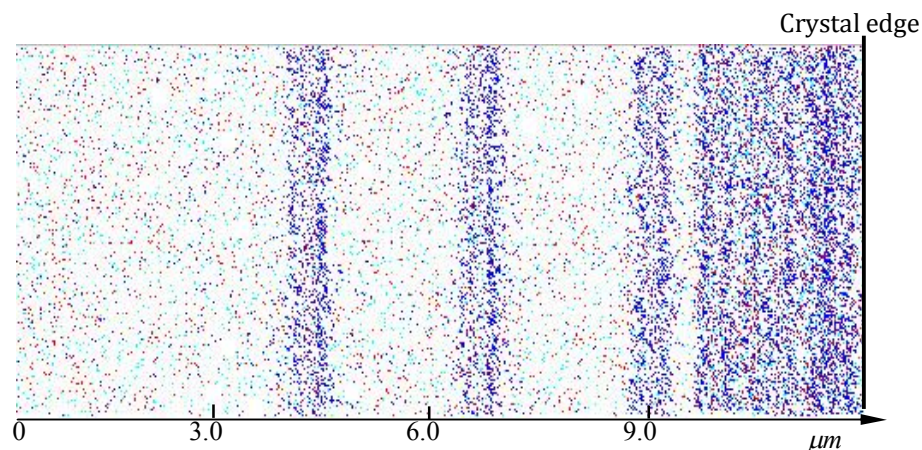


Fig. 9. Traveling wave of drifting NCs, induced by the motion of the non-stationary ILF (the meaning of colors is the same as in Fig. 4). Further explanations are in the text.

reaching the crystal edge, the NCs cannot move further and remain in place; with continuing ILF motion, new “portions” of NCs are added, etc., so that local accumulation of NCs occurs, which is reflected in Fig. 9. Due to the same mechanism, an NC-depleted region appears near the opposite (left) edge. This phenomenon is similar in its action to the motion of impurities during the zone melting method [16], and can be used for similar purposes, but much more accurately and selectively.

4. Conclusions

In this paper, we have described an efficient optical approach to the formation of controllable arrays of nanoparticles in photosensitive ACAHCs. By means of illumination of such crystals with ILF obtained by superposition of two plane waves, the simplest spatial structures are realized, and the methods for controlling the spatial distribution of quasi-metallic NCs (*X*-centers) in additively colored KCl crystals, previously tested in holographic practice [12–15], are now confirmed by the results of modeling. The approach to the formation of controllable arrays of *X*-centers, realized here using the simplest example of a spatially-structured light field, can serve as a prototype for developing refined and specialized methods for the purposeful creation of specific structures in the crystal volume, involving metallic nanoparticles obtained as products of photolysis. Since our approach is of a general nature, it can be applied to other photoconductive photochromic materials.

A direct way of further development of the results presented in this paper is associated with the involvement of more complex structured light fields for controlling the NC distributions. In this view, an interesting feature of the described SPSNCs is that quasi-metallic nanoparticles are concentrated in the minima of the ILF intensity. Accordingly, the use of singular light beams (optical vortices) [6,7,17,18] seems to be very promising, since at the singularity point the light field amplitude is close to zero. Such beams can be used to form “threads” of quasi-metallic nanoparticles [19], as well as for recording and recovering optical information on a fundamentally new basis [20].

Funding. This work was supported by the Ministry of Education and Science of Ukraine, project 610/22, #0122U001830.

Disclosure. The authors declare no conflict of interest.

References

1. Jacak, J., Krasnyj, J., Jacak, W., Gonczarek, R., Chepok, A., & Jacak, L. (2010). Surface and volume plasmons in metallic nanospheres in a semiclassical RPA-type approach: Near-field coupling of surface plasmons with the semiconductor substrate. *Physical Review B—Condensed Matter and Materials Physics*, 82(3), 035418.
2. Krenn, J. R., Dereux, A., Weeber, J. C., Bourillot, E., Lacroute, Y., Goudonnet, J. P., Schider, G., Gostschy, W., Leitner, A., Aussenegg, F. R., & Girard, C. (1999). Squeezing the optical near-field zone by plasmon coupling of metallic nanoparticles. *Physical Review Letters*, 82(12), 2590.
3. Vorob'ev, A. A. (1968). *Color centers in alkali halide crystals*. Tomsk. Gos. Univ.
4. Tyurin, A. V., Zhukov, S. A., & Akhmerov, A. Y. (2024). *Three-dimensional holographic optical elements based on new microsystems*. International Science Group.
5. Akhmerov, O., Zhukov, S. O., Savasteeva, O. M., & Tyurin, O. V. (2024). Laser guidance systems based on three-dimensional holographic optical elements. *Modern Engineering and Innovative Technologies*, (34-01), 38-49.
6. Angelsky, O. V., Bekshaev, A. Y., Hanson, S. G., Zenkova, C. Y., Mokhun, I. I., & Zheng, J. (2020). Structured light: ideas and concepts. *Frontiers in Physics*, 8, 114.
7. Bekshaev, A. Y. (2010). A simple analytical model of the angular momentum transformation in strongly focused light beams. *Cent. Eur. J. Phys.*, 8, 947–960.

8. Vladimirov, D. A., Mandel, V. E., Popov, A. Y., & Tyurin, A. V. (2004). Photothermal Conversion of F centres in Additively Coloured Potassium Chloride Crystals with Cationic and Anionic, mpurities. *Ukr. J. Phys. Opt.*, 5(4), 131.
9. Shalimova, K. V. (1985). *Physics of semiconductors*. Energoatomizdat, Moscow.
10. Popov, A. Y., Tyurin, A. V., Smyntyna, V. A., & Grinevich, V. S. (2011, 12–15 May 2011). *3D structures from nanoparticles formation by light-gradient method*. Advances in Applied Physics & Material Science “APMAS 2011”, Turkey, Antalya. Book of Abstracts: vol. 2, 445.
11. Popov, A. Y., Tyurin, A. V., & Vladimirov, D. A. (2003). Computer modeling of the photoinduced diffuse-drift instability in spatially-periodic light fields. *Visnyk Cherkas'koho Universytetu, Ser. Fiz.-Mat. Nauky*, 53, 122–131.
12. Popov, A. Y. (1995). *Photostimulated processes in alkali-halide crystals and chalcogenide glassy semiconductors upon recording volume holograms*. [Unpublished dissertation], Chernivtsi National University, Chernivtsi.
13. Belous, V. M., Mandel, V. E., Popov, A. Y., & Tyurin, A. V. (1999). Mechanism of holographic recording based on photothermal transformation of color centers in additively colored alkali halide crystals. *Optics and Spectroscopy*, 87(2), 305-310.
14. Popov, A. Y., Popova, E. V., & Tyurin, A. V. (1995). Mechanism of the FM transformation of color centers in potassium chloride crystals. *Optics and Spectroscopy*, 78(3).
15. Vladimirov, D. A., Mandel, V. E., Popov, A. Y., & Tyurin, A. V. (2005). Optimization of the recording conditions for holograms recorded in additively colored KCl crystals. *Optics and Spectroscopy*, 99, 137-140.
16. Pfann, W. G. (1966). *Zone Melting*. John Wiley & Sons, New York.
17. Bekshaev, A. Y., & Karamoch, A. I. (2008). Displacements and deformations of a vortex light beam produced by the diffraction grating with embedded phase singularity. *Optics Communications*, 281(14), 3597-3610.
18. Bekshaev, A., Sviridova, S., Popov, A., Rimashevsky, A., & Tyurin, A. (2013). Optical vortex generation by volume holographic elements with embedded phase singularity: Effects of misalignments. *Ukrainian Journal of Physical Optics*, 14(4), 171-186.
19. Bekshaev, A. Y., Karamoch, A. I., & Popov, A. Y. (2008, June 23–28). *Generation of vortex light beams by holographic grating with embedded phase singularity: output beam configuration and sensitivity to misalignments*. International Conference "Laser Optics 2008, St. Petersburg, Russia. Technical program, 29.
20. Popov, A. Y., Bekshaev, A. Y., & Tyurin, A. V. (2010, September 28–30). *Application of singular optical beams for data encoding and security*. V International Conference on Optoelectronic Information Technologies PHOTONICS-ODS 2010, Ukraine, Vinnytsia, VNTU, Abstracts, 36 (231).

A. V. Tyurin, S. A. Zhukov, and A. Y. Bekshaev. (2025). Formation of Three-Dimensional Structures of Metal Nanoparticles in Alkali-Halide Crystals Using Interference Light Field. *Ukrainian Journal of Physical Optics*, 26(3), 03043 – 03056.
doi: 10.3116/16091833/Ukr.J.Phys.Opt.2025.03043.

Анотація. Швидкий розвиток високих технологій вимагає впровадження нових способів запису, відтворення та перетворення електромагнітного випромінювання у видимому та ближньому ІЧ діапазонах. Серед них особливо актуальною є проблема створення регулярних 3D-масивів нанорозмірних об'єктів у конденсованих середовищах та керування їх властивостями, структурною і топологією. Такі нанооб'єкти та їх масиви можуть стати основою ефективних засобів керованого кодування даних та запису інформації. Зокрема, їх можна створювати в матеріалах на основі адитивно забарвлених лужно-галогідних кристалів (АЗЛГК), що містять F-центри. Переваги цих середовищ полягають у тому, що: (i) в них можна формувати нанооб'єкти вельми різноманітних структур та властивостей; (ii) просторовий розподіл квазіметалічних X-центрів, створених в об'ємі АЗЛГК внаслідок F-X-перетворення центрів забарвлення під дією інтерференційного світлового поля (ІСП), повністю відтворює його просторову структуру. Як наслідок, зміна конфігурації ІСП в об'ємі АЗЛГК дозволяє керувати просторовою структурою, утвореною X-центрами. Методи керування

просторовим розподілом X-центрів були випробувані в голографічній практиці, підтверджені результатами моделювання та можуть слугувати прототипом для широкого спектру процедур цілеспрямованої генерації структур з наночастинок, що виникають як продукти фотолізу в об'ємі кристала.

Ключові слова: *лужно-галоїдні кристали; центри забарвлення; X-центри; інтерференційне світлове поле; ефект Дембера; квазіметалічні наночастинок; тривимірні структури*